



TITLE:

Observation of excited-state excitons and band-gap renormalization in hole-doped carbon nanotubes using photoluminescence excitation spectroscopy

AUTHOR(S):

Kimoto, Yoshio; Okano, Makoto; Kanemitsu, Yoshihiko

CITATION:

Kimoto, Yoshio ...[et al]. Observation of excited-state excitons and band-gap renormalization in hole-doped carbon nanotubes using photoluminescence excitation spectroscopy. Physical Review B 2013, 87(19): 195416.

ISSUE DATE:

2013-05

URL:

<http://hdl.handle.net/2433/173928>

RIGHT:

©2013 American Physical Society

Observation of excited-state excitons and band-gap renormalization in hole-doped carbon nanotubes using photoluminescence excitation spectroscopy

Yoshio Kimoto, Makoto Okano, and Yoshihiko Kanemitsu*

Institute for Chemical Research, Kyoto University, Uji, Kyoto 611-0011, Japan

(Received 4 December 2012; revised manuscript received 19 April 2013; published 9 May 2013)

The higher Rydberg states of the E_{11} exciton in undoped and hole-doped single-walled carbon nanotubes (SWCNTs) were studied using one- and two-photon photoluminescence excitation spectroscopy. Increasing the hole-dopant concentration resulted in a redshift of the first excited state ($2g$) and a blueshift of the ground state ($1u$) of the E_{11} exciton. From the redshift of higher Rydberg states, we found that a reduction of the band-gap energy occurs in hole-doped SWCNTs. These findings show that the exciton and electronic band structures are modified by the presence of a small number of holes in the SWCNT one-dimensional structures.

DOI: [10.1103/PhysRevB.87.195416](https://doi.org/10.1103/PhysRevB.87.195416)

PACS number(s): 78.67.Ch, 71.35.-y, 78.55.-m

I. INTRODUCTION

The optical properties of semiconducting single-walled carbon nanotubes (SWCNTs) have been under intense investigation over the past decade from the viewpoints of fundamental physics and potential device applications.¹⁻³ Electrons and holes are strongly confined in the one-dimensional (1D) SWCNT structures of about 1 nm diameter. The strongly correlated electrons and holes form stable excitons with large exciton binding energies of several hundreds of meV.⁴⁻⁶ They also exhibit unique and interesting optical phenomena such as quantized exciton-Auger recombination (exciton-exciton annihilation)^{7,8} and multiple exciton generation.^{9,10} Very recently, positively charged excitons, which are one of the many-particle bound states, were discovered in SWCNTs by hole doping.¹¹ These observations of multiple exciton processes and exciton complexes indicate that SWCNTs are an excellent platform for studying many-body effects of excitons on the optical responses of 1D semiconductor quantum wires.

Extensive theoretical and experimental studies have been carried out elucidating the many-body effects of excitons in various semiconductor materials including bulk crystals and nanostructures.¹²⁻¹⁴ One intriguing phenomenon resulting from many-body effects in semiconductors is band-gap renormalization (BGR), where the band-gap energy is modified by high-density excitons or carriers. BGR has been theoretically and experimentally studied in various 1D semiconducting wire systems including SWCNTs.¹⁵⁻²² However, no conclusive experimental observations of BGR in 1D wires, even in the high-density carrier region, have been reported.^{18,19} Optical transitions in 1D wires are concentrated in the lowest exciton state and the band-to-band absorption is very weak in the linear absorption spectra,^{1,23} which makes BGR hard to observe. Almost all previous studies examining BGR in 1D wires were carried out using sophisticated GaAs-based quantum wires, which have very small exciton binding energies on the order of 10 meV.¹⁹ Thus the band-gap energy shift in 1D wires cannot be easily determined using simple optical absorption methods. However, it is expected that SWCNTs with large exciton binding energies will exhibit large shifts in the band-gap energies by carrier doping.¹⁴ Thus experimental determination of the band-gap energies for carrier-doped SWCNTs is very important for many-body physics in 1D materials and nanotube device applications.

In this paper, we report the higher Rydberg exciton and band-gap energies for hole-doped SWCNTs studied using one- and two-photon photoluminescence excitation (PLE) spectroscopy. As the dopant molecule concentration is increased, a slight blueshift in the ground state of the E_{11} exciton and significant redshift in the first excited state are observed. This finding clearly shows that band-gap shrinkage occurs due to hole doping. This remarkable result, that only a few holes modify the excited exciton and band-gap energies, opens up a new research field in 1D systems.

II. EXPERIMENT

SWCNTs were synthesized using the HiPCO and CoMoCAT methods and dispersed in toluene solutions with 0.3 wt % poly[9,9-dioctylfluorenyl-2,7-diyl] (PFO).²⁴ Moderate bath sonication was carried out for 60 min, followed by 5 h of vigorous sonication with a tip-type sonicator. Ultracentrifugation was then performed at 18 500 g for 90 min. The pristine SWCNT samples were used as undoped ones. 2,3,5,6-tetrafluoro-7,7,8,8-tetracyanoquinodimethane (F_4 TCNQ) in a 1 mg/ml toluene solution was used as a p -type dopant.²⁵

PLE spectroscopy was used to determine the higher Rydberg exciton energies and the band-gap energy of SWCNTs. PLE spectroscopy is a powerful tool for probing the higher electronic structure of a material.^{4-6,26-28} One-photon PLE spectra of the E_{11} photoluminescence (PL) intensity were obtained using a tunable Ti-sapphire laser (700–1000 nm) and a liquid nitrogen cooled InGaAs diode array. Two-photon PLE spectra were performed using a wavelength-tunable femtosecond laser system (200 fs pulse duration and 200 kHz repetition rate) and a cooled InGaAs photomultiplier with a conventional time-correlated single-photon counting setup. In the two-photon PLE measurements, the uncertainty of the peak energy, which is determined by the single Lorentzian fitting procedure, was about 0.5 meV. All experiments were carried out at room temperature.

III. RESULTS AND DISCUSSION

Figure 1(a) shows the absorption spectra of undoped CoMoCAT and HiPCO SWCNT samples. The absorption spectrum of the CoMoCAT sample is offset for clarity. A single strong peak at 1.184 eV is clearly observed in the

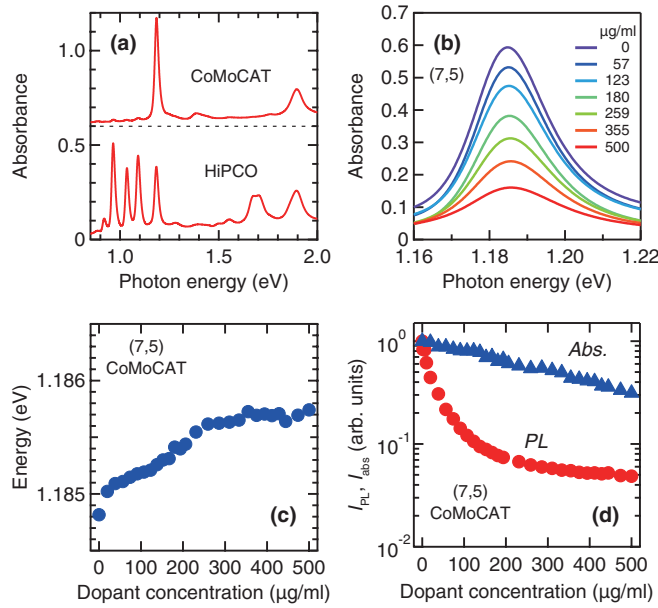


FIG. 1. (Color online) (a) Absorption spectra of undoped CoMoCAT and HiPCO SWCNT samples. The dashed line represents the offset of the CoMoCAT sample. (b) Dopant concentration dependence of the absorption spectrum of (7,5) SWCNTs in the CoMoCAT samples. (c) Dopant concentration dependence of the E_{11-1u} exciton energy of (7,5) SWCNTs in the CoMoCAT samples. The uncertainty in the fitting procedure is smaller than the plotted symbols. (d) Dopant concentration dependence of the spectrally integrated PL (filled circles) and absorption (filled triangles) intensities.

CoMoCAT sample. This peak is assigned to the $1u$ state of the E_{11} exciton (hereafter, E_{11-1u} state) for (7,5) SWCNTs.²⁴ No significant absorption peaks originating from SWCNTs with other chiralities are observed. The absorption spectrum of the HiPCO sample has five large absorption peaks in the 0.9–1.2 eV region. They appear at 0.920, 0.965, 1.035, 1.092, and 1.185 eV, respectively. These peaks correspond to the E_{11-1u} states for (9,7), (8,7), (8,6), (7,6), and (7,5) SWCNTs.²⁴ Undoped SWCNT samples with a maximum absorbance of about 0.5 were used for all measurements.

Figure 1(b) shows the absorption spectra of the E_{11-1u} state for (7,5) SWCNTs as a function of F₄TCNQ dopant concentration. As the dopant concentration increases, the peak intensity strongly decreases and a small shift in the peak position to higher energies is observed. The absorption peak without tails can be approximately fitted by a single Lorentzian function, although asymmetrical tails are considered to be due to the intrinsic exciton-phonon scattering^{29,30} and extrinsic factors such as SWCNTs with other chiralities. Then, the peak energies in the absorption spectrum for the E_{11-1u} state were determined from Lorentzian functions. Figure 1(c) shows the E_{11-1u} exciton peak as a function of the dopant concentration. The shift in energy for this range of dopant concentrations is small. The blueshift of the E_{11-1u} state by carrier doping was previously reported for a single SWCNT in the field-effect transistor (FET) structure.³¹ Our results imply that the number of holes here due to chemical doping is small.

Figure 1(d) shows the dopant concentration dependence of the spectrally integrated PL (filled circles) and absorption (filled triangles) intensities.

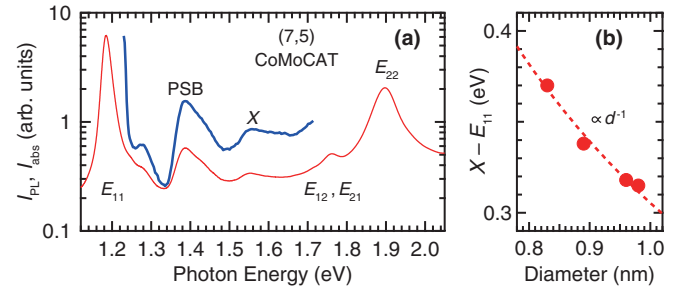


FIG. 2. (Color online) (a) Linear absorption (red curve) and one-photon PLE (blue curve) spectra for (7,5) SWCNTs in the undoped CoMoCAT sample. (b) Diameter dependence of the energy difference between the E_{11-1u} state and the X peak. The dashed line corresponds to $1/d$ dependence.

(filled triangles) intensities of (7,5) SWCNTs in the CoMoCAT samples. As the dopant concentration increases, the PL and absorption intensities decrease. The decrease in PL intensity is much stronger than the corresponding decrease in absorption intensity. This indicates that quenching of the PL intensity arises from both a decrease in absorption and an increase in nonradiative recombination caused by hole doping.

Figure 2(a) shows the absorption (red curve) and one-photon PLE (blue curve) spectra of (7,5) SWCNTs in the undoped CoMoCAT sample. Two large peaks are observed in the absorption spectrum at 1.18 and 1.90 eV, which correspond to the E_{11-1u} and E_{22-1u} exciton states, respectively. The one-photon PLE spectrum was measured in the energy region between the E_{11-1u} and E_{22-1u} exciton states. The PLE and absorption spectra are almost identical in this region. Three significant peaks appear at 1.39, 1.55, and 1.76 eV. The peaks at 1.39 and 1.76 eV correspond to the excitonic phonon sideband (PSB)³² and the transverse exciton states (E_{12} and E_{21}),³³ respectively. The E_{12} and E_{21} correspond to the optical transitions of exciton states consisting of different electron and hole subbands. The origin of the peak at 1.55 eV (labeled as X; hereafter the X peak) has not been discussed so far in ensemble samples. We also observed the X peak in (8,7), (8,6), and (7,5) SWCNTs in the HiPCO sample between the E_{11-} and E_{22-1u} exciton states.

The energy differences between the X peak and E_{11-1u} state as a function of the SWCNT diameter d are shown in Fig. 2(b). The energy difference is inversely proportional to d (dashed line), which indicates that the X peak does not originate from other phonon sidebands. Since the exciton binding energy has a $1/d$ dependence,³⁴ it is suggested that the broad X peak is intrinsic higher exciton states such as the E_{11-3u} state or the band-edge energy. An inherent characteristic of 1D excitons is that both the oscillator strengths and exciton binding energies of higher Rydberg states are extremely small.^{1,23,35} Therefore, higher Rydberg states appear as continuous states in the vicinity of the band edge in undoped and carrier-doped SWCNTs.^{35,36} The band edge can be approximated by the X peak. Note that a similar peak due to the band edge has been reported in a suspended SWCNT.²⁷ As the dopant concentration increases, the PL intensity decreases and then the Raman signal intensity is comparable with the PL intensity. Raman signals obscure the energy shift of the X peak in

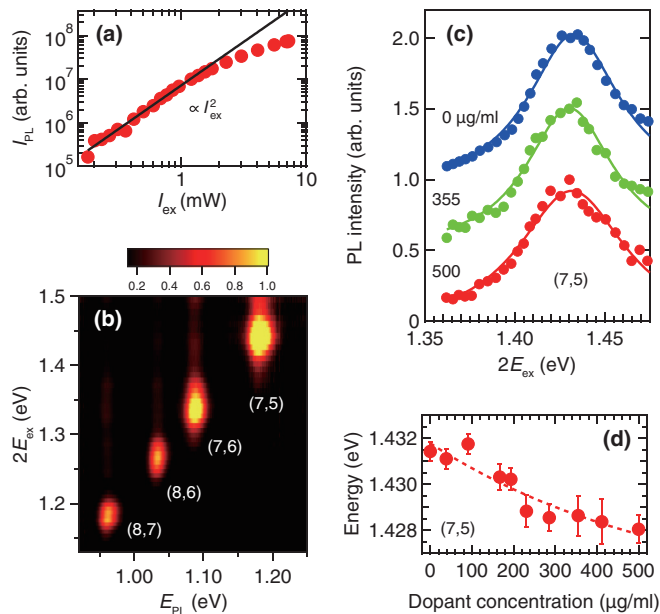


FIG. 3. (Color online) (a) Excitation power dependence of the two-photon excited PL intensity of (7,5) SWCNTs in the undoped CoMoCAT sample. The solid line represents the square of the excitation power (I_{ex}^2). (b) Two-photon PLE contour map of the undoped HiPCO sample. (c) Dopant concentration dependence of the two-photon PLE spectra for (7,5) SWCNTs in the CoMoCAT samples. The solid lines are Lorentzian fits to the data. (d) Dopant concentration dependence of the E_{11-2g} exciton energy for (7,5) SWCNTs. The error bars are determined by the experimental scatter and the uncertainty in the fitting procedure. The dashed line is a guide for the eye.

hole-doped SWCNTs. Therefore, we need to use another method for determining the band-gap energy of hole-doped SWCNTs.

In direct-gap semiconductors, the exciton binding energy and the band-gap energy are usually determined from observations of the ground and excited exciton peaks.^{37,38} In SWCNTs the band-gap energy can also be evaluated from two-photon PLE measurements of the two-photon optically allowed first excited state of the E_{11} exciton (hereafter, E_{11-2g} state).^{5,6} For two-photon PLE measurements, the excitation power dependence of the PL intensity was carefully checked. Figure 3(a) shows the PL intensity of the undoped (7,5) SWCNT sample for excitation at $2E_{ex} = 1.43$ eV. For intensities below 1.1 mW the PL intensity is proportional to the square of the excitation power. As a result, all two-photon PLE measurements were performed at intensities below 1.1 mW. Figure 3(b) shows a two-photon PLE map of the HiPCO sample. The PL signals from different SWCNTs in the HiPCO sample are distinguishable from each other using two-photon PLE techniques.

Figure 3(c) shows the dopant-concentration dependence of the two-photon PLE peak for (7,5) SWCNTs in the CoMoCAT samples. Based on the optical transition selection rules, this peak corresponds to the E_{11-2g} state.⁴⁻⁶ The positions of the peak energies for the E_{11-2g} state in hole-doped SWCNTs are evaluated by fitting the data with a single Lorentzian function (solid lines) in the range 1.35–1.47 eV, where the higher

excited exciton states and band-to-band transitions cause a tail in the PLE spectrum at the high-energy region above 1.5 eV. The peak positions for the (7,5) SWCNTs are plotted as a function of dopant concentration in Fig. 3(d). The energy of the E_{11-2g} state is slightly redshifted as the dopant concentration is increased. The shift in the peak for the E_{11-2g} state is opposite in direction to that of E_{11-1u} state.

The band-gap energy can be evaluated from the relationship between the E_{11-1u} and E_{11-2g} states,^{5,6}

$$E_g = E_{1u} + \alpha(E_{2g} - E_{1u}), \quad (1)$$

where E_g is the band-gap energy, E_{1u} is the E_{11-1u} state energy, E_{2g} is the E_{11-2g} state energy, and α is a constant. The value of α in Eq. (1) has been calculated theoretically.^{5,6,35} For undoped SWCNTs the mean value is approximately 1.4. Using $\alpha = 1.4$, the band-gap energies of SWCNTs in the CoMoCAT and HiPCO samples were evaluated. The resulting band edge energy is very close to the X peak energy observed in the one-photon PLE spectra. This result supports the conclusion that the X peak corresponds to the band gap of the E_{11} subband and enables the derivation of accurate α values for a variety of SWCNTs. For undoped SWCNTs α lies between 1.4 and 1.5, which is consistent with the theoretical calculations^{6,35} [see Fig. 4(a)]. Figure 4(b) shows the dopant concentration dependence of the band-gap energy shrinkage ΔE_g evaluated from Eq. (1) using $\alpha = 1.49$ for (7,5) SWCNTs. The reduction in the band gap is approximately 5 meV at a dopant concentration of 400 $\mu\text{g/ml}$.

Hereafter, we consider the origin of the energy shifts of the exciton states and the shrinkage in the band gap for hole-doped SWCNTs. In general, the energy shifts of the exciton states due to the change in the Coulomb interaction are determined by the self-energy corrections and the reduction of the exciton binding energies.^{1,21} In SWCNTs, the carbon atoms exist on the surface of the structure. The electronic structure of SWCNTs is therefore strongly affected by the surrounding environment.^{26,27,36,39} If the dielectric constant of the surrounding material changes, the exciton states (e.g., E_{11-1u} and E_{11-2g} states) shift in the same direction as previously reported experimentally and theoretically.^{27,36} However, in our experiments, where the surrounding environment was a solvent, the E_{11-1u} and E_{11-2g} states shift in opposite

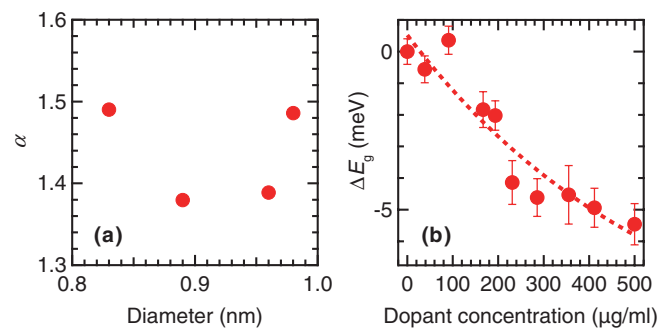


FIG. 4. (Color online) (a) Ratio of the binding energy of E_{11-1u} to the difference in energy between the E_{11-1u} and E_{11-2g} states for various SWCNTs. (b) Dopant concentration dependence of the band-gap energy shrinkage ΔE_g estimated by Eq. (1) using the two-photon PLE measurements. The dashed line is a guide for the eye.

directions upon hole doping. This result cannot be explained considering only changes in the dielectric constant of the solution in which the SWCNTs are suspended. It was also reported that mechanical strain causes a change of the band structure of SWCNTs.⁴⁰ However, in SWCNTs, a strain induces an energy shift of the E_{11} -1u state and the band gap into the same direction⁴¹; therefore, it is unlikely that the strain effect is the origin of the observed energy shifts. On the other hand, the observation that the E_{11} -1u and E_{11} -2g states shift in opposite directions upon hole doping is consistent with theoretical calculations that consider dynamical screening induced by hole doping.²¹ The calculation implies that the reduction of the binding energy of the E_{11} -1u state is larger than that of the self-energy. Therefore, we attributed the blueshift of the E_{11} -1u state and the shrinkage of the band gap to screening of the Coulomb interaction by the injected holes.

Finally, we evaluate the hole density in doped SWCNTs and discuss the band-gap shrinkage in SWCNTs. Evaluation of the number of holes, due to chemical doping, in SWCNT solutions is a difficult process. Thus we evaluate the hole density in our samples by comparison with single SWCNTs in the FET measurements.³¹ Assuming that the reduction in the PL intensity observed in the FET measurements corresponds to the reduction in the absorption intensity observed in our measurements, the hole density is estimated to be about $1.5 \times 10^{-2} \text{ nm}^{-1}$ for a dopant concentration at $400 \text{ } \mu\text{g/ml}$. This corresponds well to femtosecond transient absorption measurements where the hole density is estimated to be about $1.5 \times 10^{-2} \text{ nm}^{-1}$ for the same doping concentration,⁴² assuming that the exciton excursion range in SWCNTs is about 100 nm ,⁴³ and indicates that the band-gap shift in SWCNTs results from a small number of holes. The renormalized band-gap energy of 1D wires was numerically calculated as a function of the electron-hole (e - h) pair density, using the self-consistent screened T-matrix approximation and the screened Hartree-Fock (HF) approximation.²² This calculation predicts that a reduction in the band-gap energy starts at $n/a_{1D} = 0.01$, where n is the e - h pair density and a_{1D} is the exciton size.²² In (7,5) SWCNTs, with an exciton size of 1.4 nm ,⁴⁴ a band-gap shift is expected for low e - h pair densities around $1.4 \times 10^{-2} \text{ nm}^{-1}$. This estimated value of

e - h pairs is roughly coincident with the number of holes in our experiments, and therefore our conclusion seems to be plausible. Moreover, in 1D systems such as SWCNTs, we need to consider the charge imbalance effects.⁴⁵ In highly uniform 1D GaAs quantum wires, electron doping causes a large BGR even at low electron densities,⁴⁵ while no significant BGR is observed under photoexcitation.¹⁹ A large BGR is caused by charge carrier doping rather than photodoping of e - h pairs. Furthermore, it was theoretically shown that strong dynamical screening effects due to acoustic plasmons cause a very large BGR in hole-doped SWCNTs.²¹ These experimental and theoretical studies support that SWCNTs show large band-gap energy shifts by hole doping. However, the theoretical calculations for BGR were believed to be valid only for 1D nanowires with high-density e - h pairs²² and SWCNTs with high-density carriers.²¹ Our study shows that a small number of holes can modify the exciton and electronic band structures of 1D SWCNTs. It is believed that the band-gap energy shift is very sensitive to the number of holes and the hole-number distribution in the sample. Unfortunately, there are no theoretical studies of band-gap shrinkage and screening effects for short 1D structures with a few particles. Our experimental study provides insights into the physics of the BGR mechanism behind semiconductor nanostructures. For a better understanding of band-gap shrinkage in SWCNTs and 1D wires, theoretical studies for a few particle effects on 1D nanowires are required.

IV. CONCLUSION

In conclusion, the ground and excited exciton states were determined for undoped and hole-doped SWCNTs using one- and two-photon PLE measurements. Increasing the dopant concentration resulted in a blueshift on the E_{11} -1u state and a redshift on the E_{11} -2g state. This indicates that a shrinkage in the band-gap energy occurs upon hole doping.

ACKNOWLEDGMENTS

We thank T. Ihara for his advice. Part of this work was supported by KAKENHI (No. 20104006 and No. 25247052), The Sumitomo Electric Industries Group CSR Foundation, and JST-CREST.

*Corresponding author: kanemitsu@scl.kyoto-u.ac.jp

¹T. Ando, *J. Phys. Soc. Jpn.* **66**, 1066 (1997).

²M. S. Dresselhaus, G. Dresselhaus, R. Saito, and A. Jorio, *Annu. Rev. Phys. Chem.* **58**, 719 (2007).

³Y. Kanemitsu, *Phys. Chem. Chem. Phys.* **13**, 14879 (2011).

⁴F. Wang, G. Dukovic, L. E. Brus, and T. F. Heinz, *Science* **308**, 838 (2005).

⁵J. Maultzsch, R. Pomraenke, S. Reich, E. Chang, D. Prezzi, A. Ruini, E. Molinari, M. S. Strano, C. Thomsen, and C. Lienau, *Phys. Rev. B* **72**, 241402 (2005); **74**, 169901(E) (2006).

⁶G. Dukovic, F. Wang, D. Song, M. Y. Sfeir, T. F. Heinz, and L. E. Brus, *Nano Lett.* **5**, 2314 (2005).

⁷F. Wang, G. Dukovic, E. Knoesel, L. E. Brus, and T. F. Heinz, *Phys. Rev. B* **70**, 241403 (2004).

⁸Y.-Z. Ma, L. Valkunas, S. L. Dexheimer, S. M. Bachilo, and G. R. Fleming, *Phys. Rev. Lett.* **94**, 157402 (2005).

⁹A. Ueda, K. Matsuda, T. Tayagaki, and Y. Kanemitsu, *Appl. Phys. Lett.* **92**, 233105 (2008); Y. Kanemitsu, *Acc. Chem. Res.* (in press), doi: 10.1021/ar300269z (2013).

¹⁰S. Wang, M. Khafizov, X. Tu, M. Zheng, and T. D. Krauss, *Nano Lett.* **10**, 2381 (2010).

¹¹R. Matsunaga, K. Matsuda, and Y. Kanemitsu, *Phys. Rev. Lett.* **106**, 037404 (2011).

¹²R. Zimmermann, *Many-Particle Theory of Highly Excited Semiconductors* (Teubner, Leipzig, 1988).

¹³C. Klingshirn, *Semiconductor Optics*, 3rd ed. (Springer-Verlag, Berlin, 2007).

- ¹⁴H. Haug and S.W. Koch, *Quantum Theory of the Optical and Electronic Properties of Semiconductors*, 5th ed. (World Scientific, Singapore, 2009).
- ¹⁵S. Benner and H. Haug, *Europhys. Lett.* **16**, 579 (1991).
- ¹⁶S. Das Sarma and D. W. Wang, *Phys. Rev. Lett.* **84**, 2010 (2000).
- ¹⁷C. Piermarocchi and F. Tassone, *Phys. Rev. B* **63**, 245308 (2001).
- ¹⁸R. Ambigapathy, I. Bar-Joseph, D. Y. Oberli, S. Haacke, M. J. Brasil, F. Reinhardt, E. Kapon, and B. Deveaud, *Phys. Rev. Lett.* **78**, 3579 (1997).
- ¹⁹M. Yoshita, Y. Hayamizu, H. Akiyama, L. N. Pfeiffer, and K. W. West, *Phys. Rev. B* **74**, 165332 (2006).
- ²⁰M. Steiner, M. Freitag, V. Perebeinos, A. Naumov, J. P. Small, A. A. Bol, and P. Avouris, *Nano Lett.* **9**, 3477 (2009).
- ²¹C. D. Spataru and F. Léonard, *Phys. Rev. Lett.* **104**, 177402 (2010).
- ²²T. Yoshioka and K. Asano, *Phys. Rev. B* **86**, 115314 (2012).
- ²³T. Ogawa and T. Takagahara, *Phys. Rev. B* **44**, 8138 (1991).
- ²⁴A. Nish, J.-Y. Hwang, J. Doig, and R. J. Nicholas, *Nat. Nanotechnol.* **2**, 640 (2007).
- ²⁵M. J. O'Connell, E. E. Eibergen, and S. K. Doorn, *Nat. Mater.* **4**, 412 (2005).
- ²⁶J. Lefebvre and P. Finnie, *Phys. Rev. Lett.* **98**, 167406 (2007).
- ²⁷J. Lefebvre and P. Finnie, *Nano Lett.* **8**, 1890 (2008).
- ²⁸M. Okano, Y. Kanemitsu, S. Chen, T. Mochizuki, M. Yoshita, H. Akiyama, L. N. Pfeiffer, and K. W. West, *Phys. Rev. B* **86**, 085312 (2012).
- ²⁹S. G. Chou, F. Plentz, J. Jiang, R. Saito, D. Nezich, H. B. Ribeiro, A. Jorio, M. A. Pimenta, G. Samsonidze, A. P. Santos, M. Zheng, G. B. Onoa, E. D. Semke, G. Dresselhaus, and M. S. Dresselhaus, *Phys. Rev. Lett.* **94**, 127402 (2005).
- ³⁰O. N. Torrens, M. Zheng, and J. M. Kikkawa, *Phys. Rev. Lett.* **101**, 157401 (2008).
- ³¹S. Yasukochi, T. Murai, S. Moritsubo, T. Shimada, S. Chiashi, S. Maruyama, and Y. K. Kato, *Phys. Rev. B* **84**, 121409 (2011).
- ³²F. Plentz, H. B. Ribeiro, A. Jorio, M. S. Strano, and M. A. Pimenta, *Phys. Rev. Lett.* **95**, 247401 (2005).
- ³³Y. Miyauchi, M. Oba, and S. Maruyama, *Phys. Rev. B* **74**, 205440 (2006).
- ³⁴V. Perebeinos, J. Tersoff, and P. Avouris, *Phys. Rev. Lett.* **92**, 257402 (2004).
- ³⁵S. Uryu, H. Ajiki, and T. Ando, *Phys. Rev. B* **78**, 115414 (2008).
- ³⁶T. Ando, *J. Phys. Soc. Jpn.* **79**, 024706 (2010).
- ³⁷S. B. Nam, D. C. Reynolds, C. W. Litton, R. J. Almassy, T. C. Collins, and C. M. Wolfe, *Phys. Rev. B* **13**, 761 (1976).
- ³⁸R. C. Miller, D. A. Kleinman, W. T. Tsang, and A. C. Gossard, *Phys. Rev. B* **24**, 1134 (1981).
- ³⁹Y. Ohno, S. Iwasaki, Y. Murakami, S. Kishimoto, S. Maruyama, and T. Mizutani, *Phys. Rev. B* **73**, 235427 (2006).
- ⁴⁰M. Huang, Y. Wu, B. Chandra, H. Yan, Y. Shan, T. F. Heinz, and J. Hone, *Phys. Rev. Lett.* **100**, 136803 (2008).
- ⁴¹T. Ando, *J. Phys. Soc. Jpn.* **73**, 3351 (2004).
- ⁴²T. Nishihara, Y. Yamada, and Y. Kanemitsu, *Phys. Rev. B* **86**, 075449 (2012).
- ⁴³F. Hennrich, R. Krupke, K. Arnold, J. A. Rojas Stütz, S. Lebedkin, T. Koch, T. Schimmel, and M. M. Kappes, *J. Phys. Chem. B* **111**, 1932 (2007).
- ⁴⁴R. B. Capaz, C. D. Spataru, S. Ismail-Beigi, and S. G. Louie, *Phys. Rev. B* **74**, 121401 (2006).
- ⁴⁵H. Akiyama, L. N. Pfeiffer, A. Pinczuk, K. W. West, and M. Yoshita, *Solid State Commun.* **122**, 169 (2002).